

FIELD MEASUREMENTS OF THE VERTICAL SHEARS FOR A DRIFT CURRENT

V. A. Dulov,¹ V. N. Kudryavtsev,¹ V. I. Shrira,²
V. E. Smolov,¹ and A. N. Bol'shakov¹

UDC 551.465.15

We describe the procedure of field experiments aimed at measuring the vertical profiles of the vectors of a drift current with the help of quasi-Lagrangian drifters. We present the data on the vertical shears of the current at depths of 0.5–5 m obtained under the conditions of neutral stratification in the upper 5-m layer of the sea in the presence of weak and moderate winds. The correspondence of the obtained data to the concept according to which the subsurface layer of the sea is regarded as a near-wall turbulent layer with Ekman current located below is analyzed. A conclusion is made that the results of measurements correspond, on the average, to the classical concepts demonstrating both the region of logarithmic sublayer and its transition into the Ekman spiral.

Introduction

The processes running on the sea surface and in the upper layer of the ocean (several meters in depth) play an extremely important role in the global ocean–atmosphere system [1, 2]. In particular, they are responsible for the exchange of momentum, energy, and substances between the ocean and atmosphere. Hence, a broad circle of problems of climatic and routine simulation requires the application of adequate parametrizations of the exchange processes. The exchange processes in the ocean involve the wind waves, turbulence, and drift currents characterized by their own vertical profiles. However, their relative role in the processes of momentum and heat exchange, as well as the correlation between these processes, remain unclear despite persistent efforts of numerous researchers [2–4]. The relatively slow advance in this field is explained by the following inherent difficulties: the realization of comprehensive and precise *in-situ* measurements is still beyond the existing technical possibilities and, at the same time, any further advances in theoretical simulation require new physical ideas.

According to the classical concepts, the subsurface boundary layer is regarded as a near-wall turbulent layer subjected to the action of Earth's rotation. Therefore, it is expected that the vertical profile of current velocity near the surface is logarithmic and, with depth, turns into the Ekman spiral specified by the coefficient of turbulent viscosity at the corresponding depth [2, 3]. However, the presence of wind waves most likely violates this simple picture. In the course of numerous *in-situ* investigations [4–7, etc.], it was demonstrated that the intensity of turbulence in the upper layer significantly exceeds the predictions of the theory of near-wall turbulence. This disagreement was explained by the generation of turbulence as a result of breaking of the wind waves. The analysis of the *in-situ* data on the shears of a drift current performed in [8] revealed the deviations of the current profile from the logarithmic law caused by the influence of wave breaking in a layer of thickness $1/k$, where k is the wave number of the spectral peak of surface waves. Parallel with breaking, there exist some other possible mechanisms of influence of waves on the phenomenon of turbulence in the upper layer [4]. Thus, in particular, the role of wave motions in the generation of turbulence remains unclear. Note that, in the pioneer works carried

¹ Marine Hydrophysical Institute, Ukrainian Academy of Sciences, Sevastopol.

² Keele University, Keele, UK.

out at the Marine Hydrophysical Institute in the 1970s, it was experimentally discovered (see, e.g., [9]) that these motions induce Reynolds wave stresses. Waves can also affect the Ekman drift current as a result of the averaged action of the Coriolis force on the particles of water participating in the Stokes wave drift [10].

In this connection, it is of interest to study the situations in which the influence of wave breaking is absent or definitely insignificant. The present work is a step made in this direction. Our main aim is to estimate the profile of vertical shear of the subsurface current velocity in the upper 5-m layer on the basis of the results of purposeful measurements under the conditions of weak winds and neutral stratification of the subsurface layer of water. In this case, wave breaking cannot affect the dynamics of the upper layer and, hence, the measurements of the vertical shears of the velocity enable us either to reveal the effect of the other mechanisms of formation of the vertical profile of the wind drift current or to show that this effect is insignificant. For comparison, we also perform a similar analysis in the presence of moderate winds. If we manage to construct a physical model of the observed vertical profile, then it would be possible to establish indirect estimates of the vertical distribution of the coefficient of turbulent viscosity which can be used in numerical models.

The vertical gradients of the velocity are especially pronounced in the immediate vicinity of the free surface, where the measurements performed by immobile rigidly fixed devices are impossible in the presence of waves. The vertical resolution of the existing *ADCP*-systems (Acoustic Doppler Current Profilers) does not enable us to measure the velocities in the layer located at depths of 0.5–1 m under the surface [11]. In estimating the current velocity according to the data of measurements by *HF*-radars, we, in fact, determine the integrals of the velocity profile multiplied by a given weight function over the vertical coordinate [12]. This means that, in order to reconstruct velocities, it is necessary to know the shape of the profile in advance. This is actually a subject of our investigations. It seems likely that a single suitable (but extremely laborious) procedure of measurements is based on the use of quasi-Lagrangian drifters. The procedure of measurements of this sort is fairly well developed in the investigations of the evolution of a layer of diurnal heating of the ocean [13, 14].

Earlier, the *in-situ* experiments aimed at the description of shears of a current with the help of Lagrangian drifters launched in the upper 1-m layer were performed mainly in lakes and in the presence of weak winds (see, e.g., [15, 16] and the references therein). The analysis of these data make it possible to conclude that the velocity profile of the drift current obeys the logarithmic law predicted by the theory of near-wall turbulence [16].

In what follows, we present the data of *in-situ* measurements obtained in the sea in the presence of waves and covering not only the logarithmic sublayer but also the region of its transition into the Ekman sublayer and analyze the agreement of the obtained results with the classical ideas.

Experiment

The experimental works were carried out in the summer periods of 2000 and 2001 near the stationary oceanographic platform of the Marine Hydrophysical Institute of the Ukrainian Academy of Science in Katsiveli (Crimea). In Fig. 1a, we present a schematic diagram of the experiments and a map of the water area. The current velocities were measured with the help of drifters launched from a motor boat at a distance of 1.5–2 km from the coast. The depths of the sea in the region of works was not smaller than 50 m. In Fig. 1b, we present the design and sizes of a drifter. The drifters were made in the form of a surface float and a drogue connected by a thin steel rope. The drogue had the form of a box without bottom. The possibility of measuring currents with the help of drifters of this sort was confirmed in [13, 14].

We used five drifters with drogues located at different depths (regulated by the length of the rope). The depths of submersion of the drogues h_i ($i = 1, \dots, 5$) specified as the distances from the geometric center of the drogue to the sea surface were equal to 0.5, 1, 2, 3, and 5 m (or 10 m), respectively. Since the effective cross section of the drogue is about 50 times larger than the cross section of the float, the drifter follows the current velocity at the depth of the drogue.

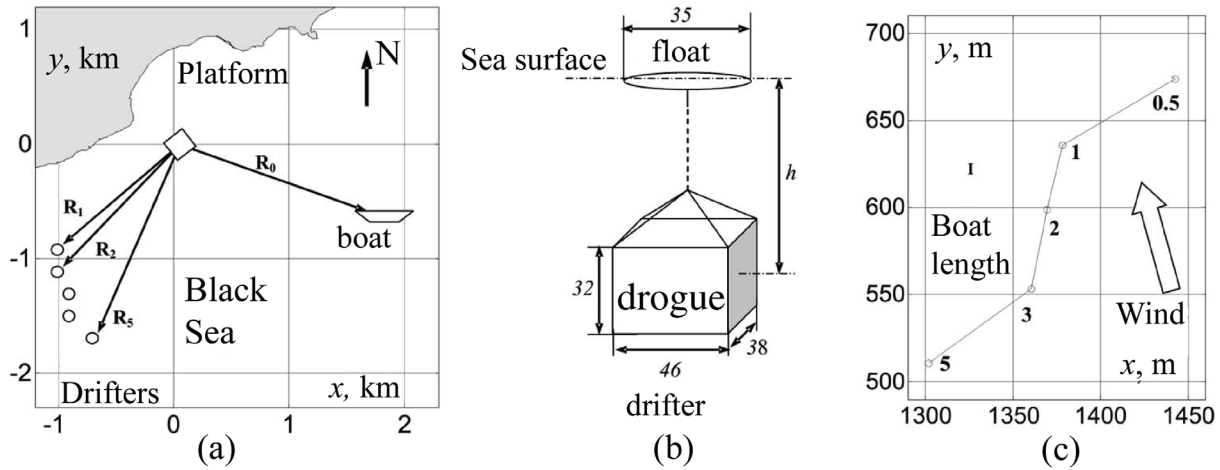


Fig. 1. Schematic diagram of experiments and a map of the water area (a), the design and sizes (cm) of a drifter (b), and an example of locations of the drifters prior to lifting (c); the numbers indicate the depths of measurements.

The procedure of measurements is illustrated in Fig. 1a. The drifters were simultaneously launched from the boat at a distance of about 2 km from the platform. The coordinates of the boat at the point of launching $\mathbf{R}_0 = (x_0, y_0)$ were determined from the platform with the help of a laser range-finder with azimuth-indicating goniometer. After a certain period of time $\Delta t = 30\text{--}60$ min sufficient for the distance between the drifters to become as large as about 100 m, the drifters were successively lifted and returned to the boat. The coordinates $\mathbf{R}_i = (x_i, y_i)$ of the places of lifting the drifters were also determined with the laser range-finder from the platform. The current velocity at the depth of the drogue was found as follows:

$$\mathbf{u}_i = \frac{\mathbf{R}_i - \mathbf{R}_0}{\Delta t_i}.$$

The mean velocity given by this formula corresponds to the actual motion only in the case where the trajectory of a drifter is close to a straight line. According to the data of visual observations, we did not detect any noticeable deviations of the motion of floats from straight lines. In Fig. 1c, we present an example of locations of the drifters prior to lifting (see experiment 27 in Table 1) and the length of the boat. As follows from Fig. 1c, the uncertainty in measuring the velocity \mathbf{u} is caused mainly by the “finite” length of the boat $l = 7$ m. Hence, for $\Delta t_i = 30$ min, the maximum error can be estimated as $\delta \mathbf{u}_i \approx l / \Delta t_i \approx \pm 4 \cdot 10^{-3}$ m/sec. For $\Delta t_i = 60$ min, the maximum error twice lower.

The measurements of currents were accompanied by recording the vertical profiles of water temperature in the upper layer with the help of an MGI-4103 (BIPT) device from the boat. From the platform, we continuously recorded the velocity and direction of a wind at an altitude of 23 m (U_{23}), the air temperature at an altitude of 11 m, water temperature, and the spectrum of waves (with the help of a resistance wave staff). The detailed description of the equipment can be found in [17]. By using the measured values of the wind velocity, water temperature, and air temperature, the friction velocity in air u_* is computed according to the method proposed in [18]. Then, in view of the condition of continuity of the flow of momentum on the sea surface, one can find the friction velocity in water v_* :

$$v_* = u_* \sqrt{\frac{\rho_a}{\rho_w}}. \quad (1)$$

For subsequent analysis, we selected the realizations obtained for the winds directed from the sea to the coast and in the case of stratification of the upper layer of water close to neutral. This means that the temperature drop in the upper 10-m layer should not exceed 0.1°C . These data do not include the effects of diurnal heating, which can significantly affect the dynamics of the upper layer for weak winds [13, 14]. Thus, we can analyze the vertical shears of current velocity caused solely by the wind action and, possibly, the action of surface waves.

Results

The conditions of the experiments are presented in Table 1, where one can find the velocity and direction of the wind, water and air temperatures, friction velocity in air, significant wave height, and the period of waves of the spectral peak. The data are gathered into two groups. The first group includes 15 current profiles obtained for weak winds with velocities not higher than 8 m/sec (the average wind velocity is equal to 6.1 m/sec). For this group of data, we can definitely state that breaking waves cannot affect the phenomenon of turbulence in the upper layer because their are either quite rare or absolutely absent (see Table 1, where we mark the cases of absence of white caps on the sea surface according to the data of visual observations). The second group of data includes 12 profiles corresponding to moderate winds with velocities of 8.1–14 m/sec (the average wind velocity is equal to 10.5 m/sec) for which the influence of wave breaking is, in principle, possible.

For the major part of realizations, the location of the drifters prior to lifting was similar to that shown in Fig. 1c. In all cases, the principal component of the transport of drifters was connected with the coastal current whose velocity was sometimes as high as 1 m/sec. In order to exclude this component from consideration, we analyzed the vector differences between the velocities of drifters 1–4 and the velocity of drifter 5 whose drogue was located at the maximum depth (10 m in experiments 1–7 and 5 m in experiments 8–27) under the assumption that the coastal current velocity is constant in the upper layer. Thus, the differences

$$\Delta \mathbf{u}_{i,5} = \mathbf{u}_i - \mathbf{u}_5, \quad i = 1, \dots, 4,$$

contain the information solely about the drift current.

In Fig. 2, we present the dependences of the modulus and direction of $\Delta \mathbf{u}_{1,5}$, i.e., of the drop of current velocity between the upper (0.5 m) and lower drifters, on the wind velocity. Here and in what follows, the direction is measured clockwise relative to the direction of the vector of wind velocity. In the plots, the direction is denoted by the word “angle.” On the average, the drop of current velocity constitutes about 1% of the wind velocity and the vector $\Delta \mathbf{u}_{1,5}$ deviates from the wind velocity to the right in agreement with the well-known empirical ideas concerning drift currents (see, e.g., a survey [10]). The data of this kind are most often characterized by a strong spread of points (cf. Fig. 8 in [15]). The mean modulus and direction of the vector $\Delta \mathbf{u}_{1,5}$ for the groups of data obtained under weak and moderate winds with mean velocities of 6.1 and 10.1 m/sec are, respectively, equal to 7.0 cm/sec, 7.2° and 8.5 cm/sec, 4.8° . This means that the modulus of the vector $\Delta \mathbf{u}_{1,5}$ increases and its direction approaches the direction of the wind as the wind velocity increases.

In Fig. 3, we present examples (experiments 9, 7, and 21 in Table 1) of measured vertical profiles of the drops of current velocity relative to the lowest depth (5 or 10 m) normalized to the wind velocity. These normalized profiles are averaged over the two groups of data corresponding to weak and moderate winds. The mean normalized profiles are shown in Fig. 4. It is easy to see that these profiles undergo systematic changes as the wind velocity increases.

Table 1. Experimental Conditions

No.	Date	Wind velocity, m/sec	Wind direction (from), degree	Air temperature, °C	Water temperature, °C	u_* , m/sec	Height of waves, m	Period of waves, sec	Presence of white caps
1	16.08.2000	5.6	97	26.0	25.8	0.17	0.2	3.0	no
2	16.08.2000	8.3	95	26.0	25.8	0.27	0.2	3.0	yes
3	16.08.2000	8.6	101	25.8	25.7	0.29	0.25	3.0	yes
4	16.08.2000	9.0	98	25.8	25.5	0.30	0.3	3.0	yes
5	16.08.2000	7.8	99	25.8	25.5	0.25	0.3	3.0	yes
6	17.08.2000	7.8	99	25.5	25.3	0.25	0.2	3.5	yes
7	17.08.2000	8.1	100	25.6	25.4	0.27	0.2	3.5	yes
8	04.09.2000	5.8	247	21.8	22.0	0.19	0.3	3.0	no
9	04.09.2000	5.7	246	22.0	22.0	0.18	0.3	3.0	no
10	04.09.2000	6.7	237	22.2	21.9	0.21	0.3	3.0	no
11	11.09.2000	5.4	101	20.3	20.9	0.18	0.1	2.0	no
12	11.09.2000	6.1	99	20.3	20.7	0.20	0.1	2.0	no
13	11.09.2000	6.0	103	20.3	20.9	0.20	0.15	2.5	no
14	11.09.2000	3.0	108	22.2	21.5	0.06	0.2	3.0	no
15	18.07.2001	10.0	87	27.5	24.3	0.30	0.47	2.8	yes
16	18.07.2001	8.0	69	26.5	24.3	0.23	0.44	3.9	yes
17	18.07.2001	5.5	148	26.9	24.4	0.12	0.48	3.5	yes
18	21.07.2001	12.5	88	30.0	24.6	0.40	0.32	2.8	yes
19	21.07.2001	13.5	93	28.6	24.5	0.46	0.32	2.8	yes
20	21.07.2001	13.0	93	28.9	24.5	0.43	0.40	3.1	yes
21	21.07.2001	14.0	93	28.3	24.6	0.49	0.43	3.1	yes
22	11.08.2001	9.1	83	28.1	26.8	0.29	0.37	4.9	yes
23	16.08.2001	8.0	103	26.8	25.9	0.25	0.23	4.1	no
24	16.08.2001	5.5	93	26.9	25.9	0.15	0.19	3.5	no
25	21.08.2001	10.0	93	26.1	25.8	0.34	0.36	3.1	yes
26	21.08.2001	10.0	93	25.9	25.6	0.30	0.35	2.5	yes
27	26.08.2001	4.0	208	26.0	25.0	0.10	0.37	4.6	no

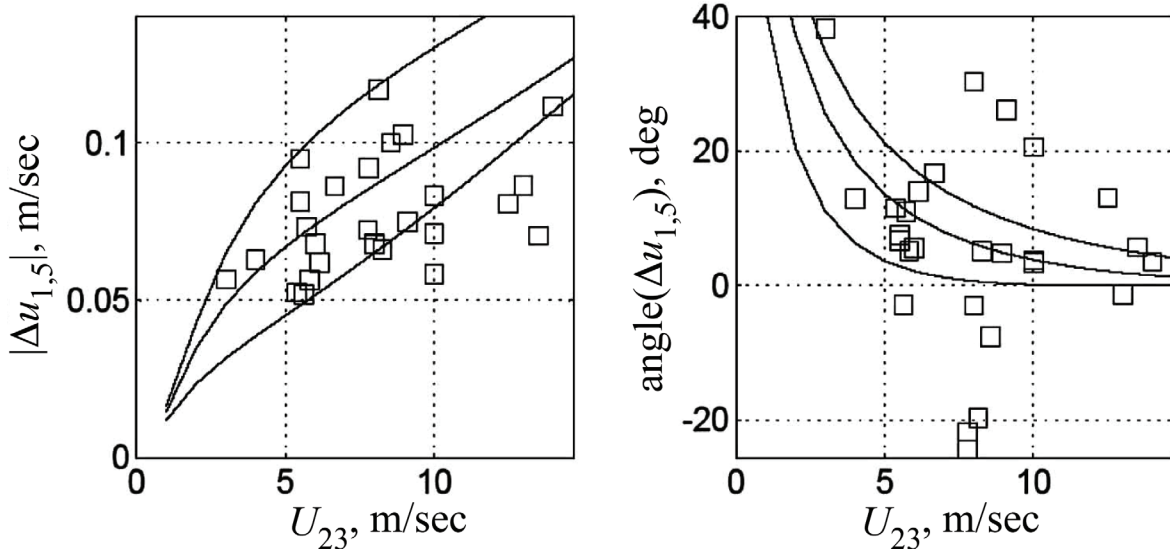


Fig. 2. Dependences of the drops of the modulus of current velocity (left diagram) and its direction (measured clockwise from the direction of the wind; right diagram) between the upper and lower drifters on the wind velocity (the squares correspond to the experimental data; the curves in the direction from the top to bottom correspond to model calculations performed for $\varepsilon = 0.1, 0.13,$ and $0.2,$ respectively).

In Fig. 5, we display the dependence of the dimensionless vertical gradient of the velocity Φ_i on the dimensionless depth. The gradient Φ_i is introduced as follows:

$$\Phi_i = \frac{\kappa z_i}{v_*} \frac{\Delta \mathbf{u}_{i,i+1}}{h_{i+1} - h_i},$$

where $\Delta \mathbf{u}_{i,i+1} = \mathbf{u}_i - \mathbf{u}_{i+1}$ is the drop of current velocity between the consecutive depths, v_* is the friction velocity in water, and $\kappa = 0.4$ is the von Kármán constant. The dimensionless depth is equal to zf/v_* , where f is the Coriolis parameter. The estimates of the gradient Φ_i are referred to the mean levels $z_i = (h_{i+1} + h_i)/2$. For each point, we find the confidence intervals determined for the maximum error of evaluation of the current velocity caused by the finite (nonzero) length of the boat. The mean relative error of the velocity gradients and the mean error of evaluation of the directions of the vectors are also presented in Fig. 5. The data obtained for weak and moderate winds are marked by different symbols. As follows from Fig. 5, there are no systematic differences between the indicated two groups of data if the results are presented in the dimensionless form.

In Fig. 6, we present the same data but after vector averaging over four groups of points lying in the consecutive intervals of dimensionless depth for which the coordinates of the boundaries increase in a geometric progression. The points are referred to the mean values of the abscissa. As confidence intervals, we use the doubled standard deviations. As follows from Fig. 6, the dimensionless vertical gradient of the velocity approaches 1 and its direction approaches the direction of the wind as the dimensionless depth decreases.

The presented data are obtained with the help of quasi-Lagrangian drifters and, strictly speaking, require corrections with regard for the Stokes drift. In our estimates, we assume that the drifters are completely entrained by the Stokes current at the depth of the center of the drogue. In this case, the contribution of the Stokes drift to the measured shear of the velocity at depth z can be estimated by the formula (see, e.g., [16, 10]):

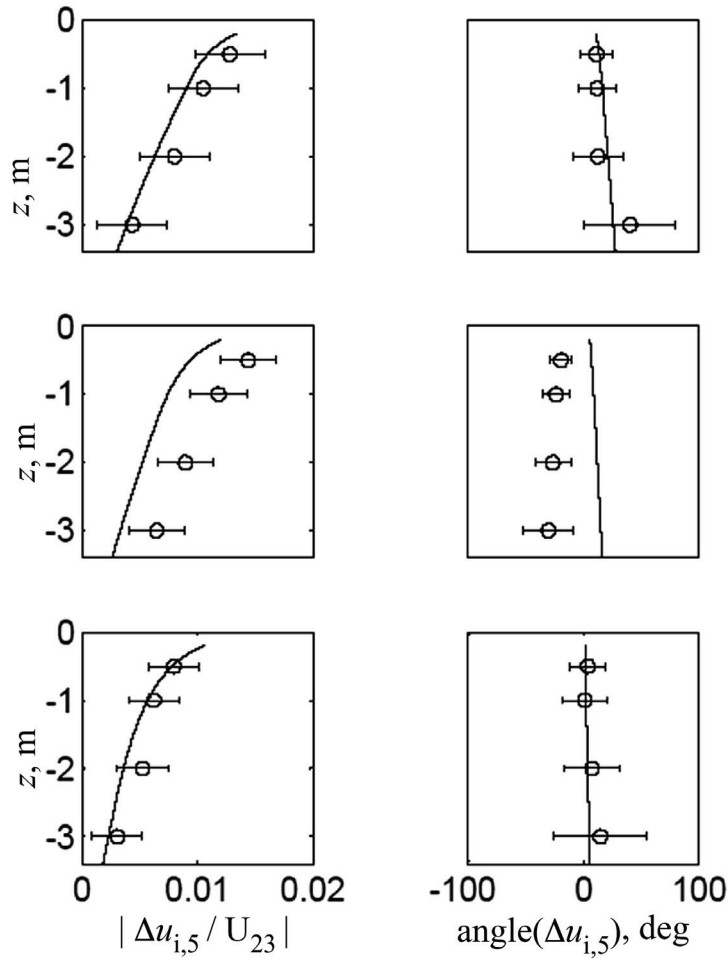


Fig. 3. Examples of the vertical profiles of shears of the current velocity (circles) relative to the lower drifter (normalized to the wind velocity). Realizations 9, 7, and 21 for the moduli (left diagram) and directions of shears (right diagram) are presented from the top to bottom (the curves correspond to the results of model calculations carried out for $\epsilon = 0.13$).

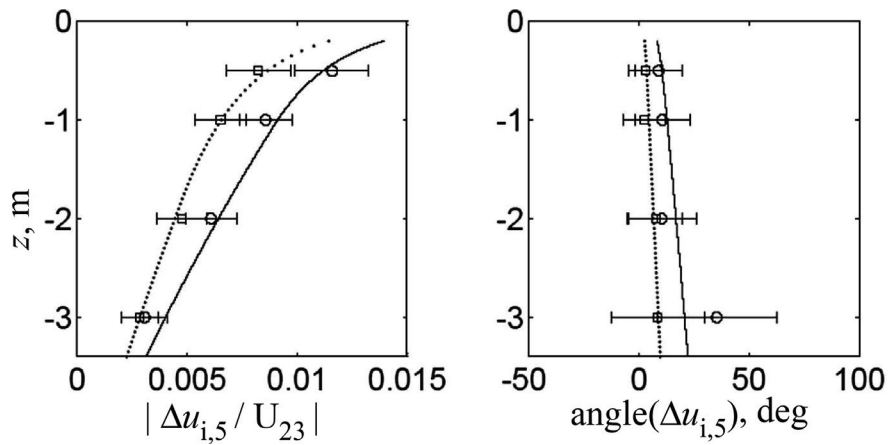


Fig. 4. Vertical profiles of the moduli (left diagram) and directions (right diagram) of mean normalized shears of current velocity relative to the lower drifter for weak (circles) and moderate (squares) winds. The continuous and dotted lines correspond to the model calculations performed for wind velocities of 6.1 and 10.5 m/sec, respectively, and $\epsilon = 0.13$.

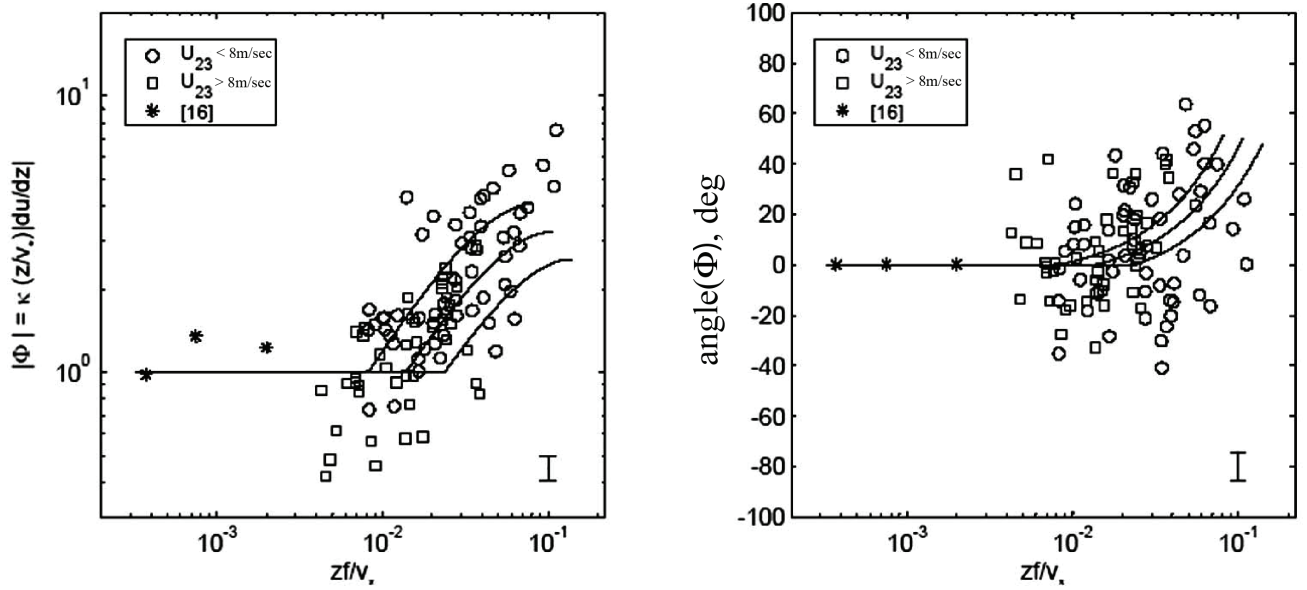


Fig. 5. Dependences of the moduli (left diagram) and directions (right diagram) of the dimensionless gradients of current velocity on the dimensionless depth for weak (circles) and moderate (squares) winds (the curves corresponding to the model calculations performed for $\varepsilon = 0.1, 0.13,$ and 0.2 are located from the top to bottom).

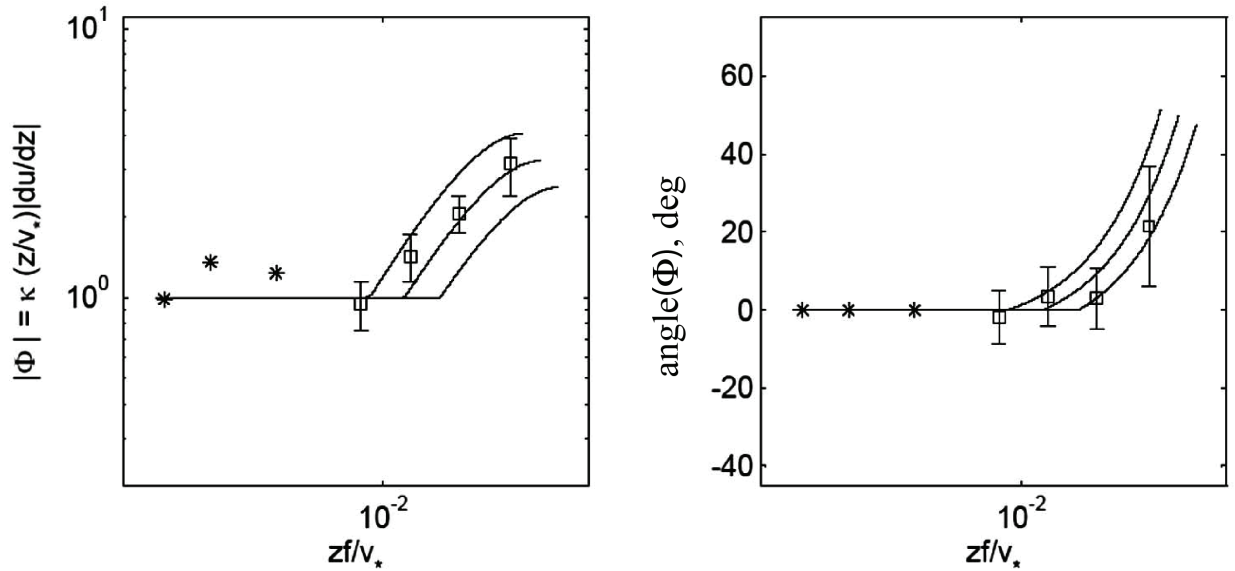


Fig. 6. The same as in Fig. 5 but the data obtained for weak and moderate winds are averaged over the consecutive intervals of dimensionless depth and marked by the squares.

$$\frac{\partial u_{\text{Stokes}}}{\partial z} = 2\omega(ak)^2 \exp(-2kz)$$

under the assumption that the amplitude a is $\sqrt{2}$ times larger than the standard deviation of the surface and the frequency ω and wave number k correspond to the spectral peak of the waves. We computed the ratio of this quantity to the actual shear of the velocity for each measured shear by using the data on the parameters of waves

presented in Table 1. The mean value of the ratio is equal to 9%. Moreover, there are only six cases in which this ratio belongs to the interval 30–70%. Thus, under the analyzed conditions, the distortions introduced by the Stokes drift to the data of measurements are insignificant.

Analysis of the Data

As a starting concept for the analysis of the accumulated data, we use a simplified model of the atmospheric planetary boundary layer proposed by Brown [19] and confirmed by the data of the *in-situ* experiments. This two-layer model consists of the logarithmic (for $z < d$) and Ekman (for $z > d$) layers. In the Ekman layer, the coefficient of turbulent viscosity K_d is independent of depth and equal to the coefficient of turbulent viscosity of the logarithmic sublayer on the boundary $z = d$. Note that, in the logarithmic layer, we have $K = \kappa u_* z$. Therefore, $K_d = \kappa u_* d$. On the boundary of the layers $z = d$, we impose matching conditions both for the velocities and their vertical gradients. These conditions enable us to determine the vertical profile of the velocity in the entire planetary boundary layer and the resistance law specifying the dependence of stresses on the geostrophic wind on the level of the underlying surface.

This model (with minimum number of modifications) can be applied to the boundary layer in the sea. In this case, we assume that, instead of the geostrophic wind velocity, the role of external parameter of the boundary layer is played by the momentum flux through the sea surface. Hence, the “resistance law” expresses the velocity vector on the surface via the indicated flux. The solution of the problem is as follows: For the profile of current velocity, we get

$$v(z) = v_s - \frac{v_*}{\kappa} \ln\left(\frac{z}{z_0}\right) \quad \text{for } z < d,$$

$$v(z) = \frac{v_*}{\kappa} \frac{1-i}{2\varepsilon} \exp\left[-\varepsilon(1+i)\left(\frac{z}{d}-1\right)\right] \quad \text{for } z > d.$$

The velocity on the sea surface is given by the formula

$$v_s = \frac{v_*}{\kappa} \left[\ln\left(2\kappa\varepsilon^2 \frac{v_*}{fz_0}\right) + \frac{1-i}{2\varepsilon} \right].$$

In these equations, v_* is the friction velocity in water given by Eq. (1), d is the depth of the logarithmic layer connected with the depth of the Ekman layer ($D = 2\kappa\varepsilon v_*/f$) by the formula $d = \varepsilon D$, f is the Coriolis parameter, z_0 is the parameter of roughness, i is the imaginary unit, and ε is a constant much smaller than 1 playing the role of a single fitting parameter of the model. For the atmosphere, this constant is equal to 0.10–0.15. Hence, the dimensionless vertical gradients of current velocity are given by the formulas

$$\frac{\kappa z}{v_*} \frac{\partial v}{\partial z} = 1 \quad \text{for } \frac{1}{2\kappa\varepsilon^2} \frac{zf}{v_*} < 1,$$

$$\frac{\kappa z}{v_*} \frac{\partial v}{\partial z} = \frac{1}{2\kappa\varepsilon^2} \frac{zf}{v_*} \exp\left[-\varepsilon(1+i)\left(\frac{1}{2\kappa\varepsilon^2} \frac{zf}{v_*} - 1\right)\right] \quad \text{for } \frac{1}{2\kappa\varepsilon^2} \frac{zf}{v_*} > 1.$$

As follows from these equations, the dimensionless vertical gradient of the velocity is a universal function of the dimensionless depth zf/v_* in agreement with the Kazanskii–Monin–Obukhov similarity theory [20].

According to the model, the depth of the logarithmic sublayer is given by the formula

$$d = \frac{2\kappa\varepsilon^2 v_*}{f} \quad (2)$$

and varies from 0.3 to 2.4 m under the analyzed experimental conditions. The corresponding depth of the Ekman layer varies within the range 2.3–20 m. Thus, the accumulated data should reveal the specific features of currents in the Ekman layer. The results of calculations performed according to the model are shown in Figs. 2–6 (in Fig. 4, one can find the data obtained for the wind velocities averaged over each of the two groups of data). It should be emphasized that, in all calculations, we determine the drops of velocities independent of the coefficient of roughness of the sea surface and, therefore, it is not necessary to determine this quantity.

As follows from Fig. 2, the model curves pass through the central parts of the clusters of points and correctly reflect their slopes, although the great spread of experimental values does not allow one to speak about definite agreement. For specific realizations in the cases of both weak and moderate winds, the observed agreement is sometimes quite good (see realizations 9 and 21 in Fig. 3). At the same time, in other cases, we reveal a well-pronounced disagreement (see, e.g., realization 7 in Fig. 3). However, the results of model calculations presented in Fig. 4 are in fairly good agreement with the averaged data and correctly describe the dependences of the vectors of shear of the velocity on the wind velocity and depth. The indicated correspondence is attained for $\varepsilon = 0.13$.

In Figs. 5 and 6, we present the computed universal dependences of the modulus and direction of the dimensionless velocity gradient Φ on the dimensionless depth. In these dependences, the logarithmic and Ekman parts of the sea boundary layer are well visible. Indeed, in the logarithmic part, we have $|\Phi| = 1$ and $\text{angle}(\Phi) = 0$. Our data correspond to the Ekman part and the region of its transition into the logarithmic part. The investigations of velocity shears at smaller dimensionless depths carried out under the *in-situ* and laboratory conditions show that the profile of the velocity modulus in this region is logarithmic and the direction of the velocity gradient coincides with the direction of the wind (see surveys [15, 16]). Since it is impossible to represent the vast array of these data in the dimensionless form, we add only three points plotted according to the data presented in [16] to Figs. 5 and 6. These points give an idea of location of a cluster of the corresponding experimental data in the coordinate planes used in the plots.

In view of the available data on the presence of a logarithmic layer, Figs. 5 and 6 show that our measurements do not contradict the model based on the classical hypothesis that the sea boundary layer can be regarded as a near-wall turbulent layer on the rotating Earth. However, the model data agree with the results of measurements only on the average. Just in this sense, the data on the moduli and directions of the gradients reveal the Ekman spiral which transforms into the logarithmic layer with dimensionless gradient equal to one and directed in the direction of the wind. This conclusion is true in the cases of both weak and moderate winds.

Note that the strong spread of data in the Ekman part of the layer is not surprising because the nonstationary character of external conditions on the scale of several hours typical of our measurements leads to the variations of the Ekman flow in the form of inertial oscillations, i.e., to the phenomena observed earlier with the help of the method of quasi-Lagrangian drifters [14]. However, we cannot explain the fact that the spread of data remains on the same level also in the logarithmic layer.

In [4–7], one can find the description of the strong action of surface waves on turbulence realized via the effect of wave breaking. In our experiments, we avoided stormy conditions. Therefore, our data on the velocity profiles should not contain the effects of wave breaking. However, in all experiments, we observed either the wind waves or swell on the sea surface. In analyzing the data, we did not reveal the action of waves on the aver-

aged current profile. At the same time, strong deviations from the averaged profile observed in specific realizations can be associated with the influence of waves on the subsurface turbulence even under the conditions of weak and moderate winds.

CONCLUSIONS

In the *in-situ* experiments carried out by using quasi-Lagrangian drifters, we obtained the vertical profiles of the vectors of shear of the velocity for a drift current in the upper 5-m layer of the sea under the conditions of neutral stratification of the layer in the presence of weak and moderate winds. The analysis of the data shows that the measured shears of the velocity are, on the average, described by using the classical concept of near-wall turbulent layer with Ekman current located below this layer. The profile of the coefficient of turbulent exchange by momentum agrees with the accumulated data and has the form

$$K = \kappa v_* z \quad \text{for } z < d,$$

$$K = \kappa v_* d \quad \text{for } z > d,$$

where v_* is given by relation (1) and d is given by relation (2) with $\varepsilon = 0.13$. For moderate winds with velocities of 8–14 m/sec, the phenomenon of breaking of wind waves, most likely, does not affect the shears of the drift current at depths not smaller than 0.5 m.

The present work was financially supported by the EC (Grant INTAS 01-234) and ESA-IAF within the framework of the program “GMES Networking with Russia and Ukraine” (OSCSAR Project).

REFERENCES

1. A. E. Gill, *Atmosphere–Ocean Dynamics*, Academic Press, New York (1982).
2. S. A. Thorpe, “Recent developments in the study of ocean turbulence,” *Annual Rev. Earth Planet. Sci.*, **32**, 91–109 (2004).
3. S. A. Thorpe, “A comparison of stable boundary layers in the ocean and the atmosphere,” *Bound.-Lay. Meteor.*, **90**, 521–528 (1999).
4. A. Anis and J. N. Moum, “Surface wave–turbulence interactions: scaling $\varepsilon(z)$ near the sea surface,” *J. Phys. Oceanogr.*, **25**, 2025–2045 (1995).
5. Y. C. Agrawal, E. A. Terray, M. A. Donelan, et al., “Enhanced dissipation of kinetic energy beneath surface waves,” *Nature*, **359**, 219–220 (1992).
6. E. A. Terray, M. A. Donelan, Y. C. Agrawal, et al., “Estimates of kinetic energy dissipation under breaking waves,” *J. Phys. Oceanogr.*, **26**, 792–807 (1996).
7. J. R. Gemmrich and D. M. Farmer, “Near-surface turbulence in the presence of breaking waves,” *J. Phys. Oceanogr.*, **34**, 1067–1086 (2004).
8. W. M. Drennan, E. A. Terray, and M. A. Donelan, “The vertical structure of shear and dissipation in the ocean surface layer,” in: M. L. Banner (Ed.), *The Wind-Driven Air-Sea Interface*, The University of NSW (1999), pp. 239–245.
9. V. V. Efimov, *Dynamics of Wave Processes in the Boundary Layers of the Atmosphere and the Ocean* [in Russian], Naukova Dumka, Kiev (1981).
10. N. E. Huang, “On surface drift currents in the ocean,” *J. Fluid Mech.*, **91**, Pt. 1, 191–208 (1999).
11. D. Ivonin, P. Broche, J.-L. Devenon, et al., “Validation of HF radar probing of the vertical shear of surface currents by ADCP measurements,” *J. Geophys. Res.*, **109**, No. C4, C04003 (2004).
12. V. Shrira, D. Ivonin, P. Broche, et al., “On remote sensing of vertical profile of ocean surface currents by means of a single-frequency VHF radar,” *Geophys. Res. Lett.*, **28**, 3955–3958 (2001).

13. V. N. Kudryavtsev and A. V. Soloviev, "Slippery near-surface layer of the ocean arising due to daytime solar heating," *J. Phys. Oceanogr.*, **20**, 617–628 (1990).
14. V. Kudryavtsev, A. Tsvetkov, and S. Grodsky, "Diurnal heating of the ocean surface layer," in: M. A. Donelan, W. H. Hui, and W. J. Plant (Eds.), *The Air-Sea Interface: Radio and Acoustic Sensing, Turbulence, and Wave Dynamics*, The University of Toronto Press, Toronto (1996), pp. 549–556.
15. J. H. Churchill and G. T. Csanady, "Near-surface measurements of quasi-Lagrangian velocities in open water," *J. Phys. Oceanogr.*, **13**, 1669–1680 (1983).
16. G. T. Csanady, "The free surface turbulent shear layer," *J. Phys. Oceanogr.*, **14**, 402–411 (1984).
17. V. A. Dulov, V. N. Bol'shakov, V. E. Smolov, et al., "In-situ investigations of the spatial homogeneity of meteorological and wavegraphic parameters in the coastal zone. On the problem of calibration of a *Sich-IM* side-looking radar used as a tool for measuring the surface wind velocity," *Morsk. Gidrofiz. Zh.*, No. 3, 31–43 (2005).
18. W. G. Large and S. Pond, "Open ocean momentum flux measurements in moderate to strong winds," *J. Phys. Oceanogr.*, **11**, 324–336 (1981).
19. R. Brown, "On two-layer models and the similarity functions for the PBL," *Bound.-Lay. Meteorol.*, **24**, 451–463 (1982).
20. A. B. Kazanskii, A. S. Monin, "On the turbulent mode over the surface layer of air," *Izv. Akad. Nauk SSSR, Ser. Geofiz.*, No. 1, 165–168 (1960).